Hindawi
Mobile Information Systems
Volume 2022, Article ID 1271190, 6 pages
https://doi.org/10.1155/2022/1271190

Research Article

Software Optimization of Welding Machine Motion System Based on Switch Control Algorithm

Jingbo Yin[1], **Xing Liu**[1], **Xunde Guo**[1] and **Lianwang Gudsla**[2]

[1]*Department of Mechanical and Electrical Engineering, Shandong Water Conservancy Vocational College, Rizhao, Shandong 276826, China*
[2]*Tengzhou Anchuan Automation Machinery Co., Ltd, Zaozhuang, Shandong 277500, China*

Correspondence should be addressed to Jingbo Yin; 147740913@st.usst.edu.cn

Received 5 May 2022; Accepted 10 June 2022; Published 22 June 2022

Academic Editor: Jiguo Yu

In order to improve the software optimization of welding machine motion system based on switch control algorithm. Based on soft switch arc welding power source current peak control the stability of the BUCK converter, the method by solving peak current control circuit transfer function, and to analyze the formation mechanism of soft switch arc welding power source external characteristic, the frequency of pulse current in the simulation model is set to 200 Hz, the base value of pulse current is 40 A, the peak value of pulse current is 500 A, and the duty cycle is 40%. The welding wire melting speed during the peak value of pulse current is 480 mm/s, while the base value of pulse current is 20 mm/s. The results show that in the 2 s moment of the simulation model, the welding torch suddenly drops from 40 mm height to 30 mm height. Inevitably, the arc length changes from about 16 mm before the step to about 6 mm, which is basically equal to the step change distance. Using pulse frequency modulation (PFM) and adaptive adjustment of pulse current related parameters, effectively eliminate the interference factors in the welding process, quickly adjust arc welding parameters to make the welding wire melting speed equal to the wire feeding speed, maintain the stability of the welding process, and improve the weld forming effect. It is of great significance to the software optimization of the motion system of the pulse welding machine.

1. Introduction

With modern computer technology, information technology, power electronics technology, and intelligent software control technology, represented by the new technology for the development of arc welding technology has brought a lot of opportunities and challenges [1], not only in the welding quality of the direction of light, small volume, high strength, and a variety of applications require stable welding process, welding quality is reliable. With the development of materials science and the progress of related technologies, welding processing has been involved in a wider range [2]. On the one hand, the welding process has become the key technology for the mass use of many new materials; on the other hand, many software engineering applications have put higher requirements for the welding process, such as high-speed welding, efficient welding, splash, and arc initiation [3]. "To do a good job, you must first sharpen its tools," welding equipment is the key link of welding production; welding equipment is the key to expand the application of welding technology, and improve the quality and efficiency of welding. The core component of welding equipment is the welding power supply, so in order to better realize various advanced welding methods, higher requirements are put forward for the research of welding power supply. Motion control system software is one of the key components in determining welding performance [4]. The motion control algorithm is the core technology to determine the characteristics of motion control system software to improve the competitiveness of the enterprise [5]. At present, arc welding has developed from a traditional thermal processing process to a comprehensive process and technology discipline integrating material science, metallurgy, mechanics, heat treatment, electronic technology,

control software engineering, inspection technology, etc. and has formed a new process method by constantly bringing forth the new and combining new knowledge and technology.

Arc welding is widely used in machinery manufacturing, metallurgy, power equipment, petrochemical industry, transportation, construction engineering, aerospace, military, and other fields, and it plays an important role in national economic construction and national defense science and technology construction [1]. In view of this research problem, Peng and Li believe that the outstanding advantages of a dual-tube forward converter circuit are that there is no danger of straight-through, no transformer magnetic bias and magnetic saturation problems, and high reliability. However, there are disadvantages of the low utilization rate of the power transformer core and large output filter inductance [6]. Liu and Feng believed that the adaptability to the change of nonlinear abrupt load such as arc was poor and the control was complicated, so it was difficult to optimize the parameters such as filter. The conduction loss and voltage and current stress of power devices increase [7]. Lim and Kim believed that during the commutation of power switching devices, the resonance principle was applied to realize the natural switching of zero voltage or zero current, while during the power transmission, constant frequency pulse width modulation (PWM) was adopted to complete the control of the inverter's output voltage or current. In essence, the commutation process of devices and time-sharing of energy conversion were differentiated [8]. In the current study is proposed in this paper, based on a soft switch arc welding power source based on the stability of the peak current controlled BUCK converter, the method, by solving the peak current control circuit transfer function of the soft switch arc welding power source external characteristic analysis; the formation mechanism of pulse current in the simulation model is set to 200 Hz frequency, pulse current base value of 40 A, the peak pulse current is 500 A, the duty cycle is 40%, the welding wire melting speed during the peak pulse current is 480 mm/s, and the base pulse current value is 20 mm/s, using pulse frequency modulation (PFM) and adaptive adjustment of pulse current related parameters, effectively eliminating the interference factors in the welding process. The arc welding parameters should be adjusted quickly to make the welding wire melting speed equal to the wire feeding speed, and the welding process should be kept stable to improve the weld forming effect [9]. A remote state Internet of Things monitoring and fault prediction system based on a custom software-defined network (SDN) technology was proposed by Eshaghzadeh et al. to transition to a smart grid by integrating a power grid and efficient real-time wireless communication architecture. The core network consists of redundant links used to recover from any future failure [10].

Innovation point of this article: the verification of the simulation dynamic law of the pulse arc welding process provides a new way for optimizing the parameter design of the actual pulse GMAW welding arc welding inverter power controller and verifying the new arc length control algorithm and strategy.

2. Methods

2.1. Arc Welding Inverter. Arc welding inverter itself is nonlinear, converter designed by the nonlinear model is difficult to achieve, needing idealized simplify the switch components, namely, ignoring conduction pressure drop and leakage current, is an ideal conversion switch, namely, on-off mutexes, transient, and disturbance signal is much smaller than the steady-state value, namely, the small signal disturbance, and the power tube frequency switching frequency is greater than the output filter. In addition, Taylor's formula was used to expand the nonlinear model of the switching inverter. High-order terms were ignored and the approximation process was carried out to obtain an approximate linearized transient small signal model, and the control theory was used for AC analysis of the system software. The overall structure of the control system is composed of high performance 16-bit MCU 80C196KC as the core, as shown in Figure 1.

2.2. Stability of BUCK Converter Current Peak Control Software. For the convenience of analysis, it is assumed that the control quantity $i_c(t)$ of the inner ring current is not affected by subharmonic oscillation (is a constant), and the inductance current waveform of the BUCK converter is shown in Figure 1. The inductance current rising slope is $m_1 = (v_g - v)/L_0$, and the inductance falling slope is $-m_2 = -v/L_0$. The variation of output inductance current is analyzed during a switching cycle. During the time $[0, \mathrm{d}T_s]$, the power switching device is on and the inductance current increases linearly. When $t = dT_s$, the inductance current $i_L(dT_s)$ is equal to the current set value i_c, as shown in the following formula:

$$\begin{aligned} i_L(dT_s) &= i_c \\ &= i_L(0) + m_1 dT_s. \end{aligned} \tag{1}$$

During the time $[dT_s, T_s]$, the power switch tube is turned off, the inductance current continues through the diode, and the inductance current decreases linearly. When $t = T_S$ is the inductance current, it is shown in the following formula:

$$i_L(T_s) = i_L(dT_s) - m_2 dT_s. \tag{2}$$

Formula (3) can be obtained,

$$i_L = i_L(0) + m_1 dT_s - m_2 dT_s. \tag{3}$$

When the current peak control mode reaches a steady state, the inductance current value at the beginning of each switching cycle should be equal to the inductance current value at the end of the switching cycle, as shown in the following formula:

$$i_L(T_S) = i_L(0). \tag{4}$$

Formula (5) can be obtained,

$$0 = m_1 dT_s - m_2 dT_s. \tag{5}$$

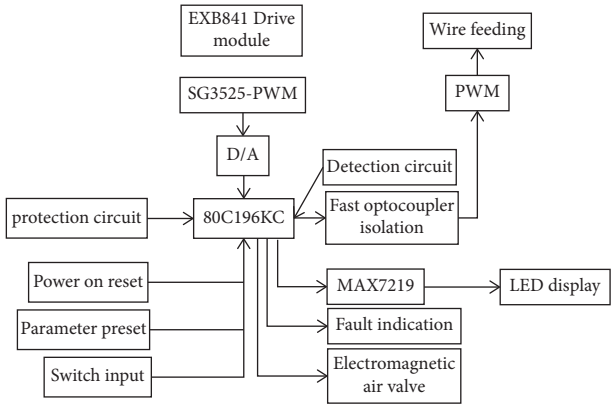

Figure 1: Block diagram of the control system software structure.

In the steady state, duty cycle D is d and D' is D', so equation (5) can be changed into the following equation:

$$\frac{m_2}{m_1} = \frac{D}{D'}. \tag{6}$$

When there is no disturbance, the initial value of the inductance current at the beginning of the switching cycle is $i_L(0) = I_{L0}$, and when $t = DT_s$, the inductance current $i_L(DT_s)$ reaches the current control value i_c. The waveform of inductance current when no disturbance occurs, the relationship between the control value of inductance current i_c and the starting value of inductance current $i_L(0) = I_{L0}$ and the space ratio D is shown in the following formula:

$$i_c = I_{L0} + m_1 DT_s. \tag{7}$$

Suppose that at time $t = 0$ there is a disturbance of inductance current, whose value is $i_L(0) = I_{L0} + \hat{i}_L(0)$, and the disturbance of duty cycle is $D + \hat{d}$. At $t = (D + \hat{d})T_s$, the inductance current reaches the current control value i_c; when $t = T_s$, the inductance current drops to $i_L(T_S) + \hat{i}_L(T_S)$. At this point, the circuit process enters the transient running state and the initial value of the inductance current in each switching cycle is not equal to the end value of the switching cycle [11]. The waveform of inductance current after the occurrence of disturbance can be seen from the relationship between the current control value i_c and the initial value $i_L(0) = I_{L0} + \hat{i}_L(0)$ of inductance current after the occurrence of disturbance and the duty cycle $D + \hat{d}$ as shown in the following formula:

$$i_C = I_{L0} + \hat{i}_L(0) + m_1(D + \hat{d})T_S. \tag{8}$$

The inductance current disturbance $\hat{i}_L(T_S)$ at the end of a switching cycle equals the product of the inductance current disturbance $\hat{i}_L(0)$ at the beginning of the switching cycle and the factor $(-m_2/m_1)$, as shown in the following formula:

$$\hat{i}_L(T_S) = \left(-\frac{m_2}{m_1}\right)\hat{i}_L(0). \tag{9}$$

The criterion for evaluating the stability of the current inner loop is: with the increase of N, the disturbance quantity should eventually decrease to zero; that is, the disturbance is suppressed or eliminated by the current inner loop. Generally, from the angle of the main circuit power transformation optimization, hope the switch duty ratio is greater than 0.5, designed to help improve the efficiency of the power converter, and reduce output ripple; however, the peak current control mode stability conditions and clashes between converter main circuit optimization design, the technique of artificial slope compensation is an effective method to solve this contradiction [12]. The model of pulse GMAW arc welding is related to realize the stable melting droplet transition and arc length stability control of pulse GMAW welding.

2.3. Formation Mechanism of External Characteristics of Soft Switch Arc Welding Power Supply. Under certain internal parameters of the soft-switch arc welding inverter, the relationship curve between the stable output voltage U_0 and the stable output current I_0 of the power supply is the external characteristics, namely, the static characteristics of the arc welding inverter by changing the load. The external characteristics of arc welding inverter are a series of curve families. Among them, the relation curve between the maximum voltage stable value $U_{\max}$ output by the inverter power supply and the current stable value I_0 is the external characteristic boundary of arc welding inverter [13]. The boundary of external characteristics determines the adjustment range of output welding process parameters of arc welding inverter, and the boundary parameters determine the arc starting voltage, maximum output power, short circuit transition characteristics, and other key indicators of arc welding power supply. In order to design to the qualitative and quantitative analysis of structural parameters of soft switch arc welding inverter and external characteristic mechanism, essentially soft switching full bridge phase shift converter can be equivalent to exist a certain duty ratio loss of BUCK converter, and vice side duty cycle loss is the full bridge phase shifting soft switch inverter converter one common feature, is the resonance soft switch converter produces; due to the existence of transformer leakage inductance L_r Lr, during the resonant process $[t_1, t_4]$, although Q_1, Q_4 is in the on-state, the inductance current can only rise linearly to the forward I_1. The transformer secondary is short-circuited to the transformer primary due to current commutation, resulting in the effective duty cycle loss of ΔD, and the slope of the primary current rise during $[t_2, t_4]$ is $U_S/L_r = U_{\text{in}}/(nL_r)$. The slope of primary current rise during $[t_4, t_5]$ is $(U_{\text{in}} - nU_0)/(n^2L_0 + L_r)$, where I is transformer primary current, U_0 is inverter output voltage stability value, D is primary effective duty cycle, D_{eff} is secondary effective duty cycle, N is power transformer primary stage change ratio, I_P is primary current maximum, t is time, T_S is converter switching cycle, U_S is the secondary output voltage of the transformer, and $I_L = U_0/R_L$ is the load current. When I_L is 0, U_0 is no-load voltage. When the output current I_L is small, the output inductance current is discontinuous, so it can be seen that the rate of change of $\Delta U/\Delta I$ is large. With the increase of load current I_L, the stable value of output voltage U_0 decreases rapidly. The

above-given statement qualitatively explains the upturning boundary of external characteristics of arc welding inverter theoretically. When the output current I_L reaches a certain value, the output inductance current works in a continuous state, and it can be seen that the change rate of $\Delta U/\Delta I$ is constant. Therefore, the natural slow drop section of the external characteristic boundary of the soft switch arc welding inverter is approximately a straight line segment [14].

The external characteristic boundary of the power supply is composed of three sections: upwarping section AB, slow falling section BC, and constant current section CD. Which point A said the no-load voltage of inverter power supply, the high no-load voltage of arc process quickly built, point B is the output inductor current is A continuous state (DCM) and continuous state (CCM) critical point, and the BC segment for an arc state transition to A stable state of the arc welding process, approximate to the constant voltage output, the process to maximize the PWM inverter output. To reach the set working current at the fastest speed, point C represents the maximum constant current welding specification of the arc welding inverter, and section CD represents an approximate constant current process, which makes the arc welding process have high stability. Because become warped in arc welding inverter and natural slow down section, PWM modulator is working in the largest conduction state and the output is constant conduction ratio, so the external characteristic and natural slow drop become warped on the boundary is has nothing to do with structural parameters of the conduction than modulator, also has nothing to do with the main circuit control mode, only depend on arc welding inverter main circuit topology structure and related parameters [15]. The external characteristic constant current boundary, the conduction ratio regulator of arc welding power inverter works in a linear state, and the constant current boundary is the result of feedback control mode and main circuit parameters. Based on double closed-loop peak current, average current control inverter and the inner ring peak current feedback mode setting maximum peak current of the transformer, to prevent damage of transformer magnetic saturation and switch tube flow plays a key role, but the inner ring peak feedback unable to precisely adjust the secondary side rectifier current output size must add outer ring average current feedback mode. Only in this way can the actual filtered output current-load current of the inverter be precisely controlled, so as to ensure the realization of the constant current boundary of external characteristics [16].

3. Results and Analysis

By analyzing the working timing of MAX7219, the top 8 are used to select the internal register address of MAX7219, and the last 8 are the command or displayed content. In the simulation model, pulse current frequency is set as 200 Hz, pulse current base value is 40 A, pulse current peak value is 500 A, the duty cycle is 40%, and welding wire melting speed during the peak pulse current is 480 mm/s, while the base value of pulse current is 20 mm/s; welding wire melting process mainly occurs during the peak pulse current. With the known as the pulse welding pattern: in the peak current pulse phase of the molten solder wire and form a droplet transition, base value and pulse current period keep d arc principle is consistent, but in the whole process of pulse cycle of welding wire melting rate is equal to the set value of wire feeding speed 200 mm/s, namely, in the process of welding wire melting speed and the welding wire feed speed to keep dynamic balance. According to the principle of real-time energy, in a single pulse cycle as long as the average of a certain welding current, arc length due to the adjustment type dynamic model of the pulse frequency is fixed, know basic constant pulse current of power, so welding wire melting rate is constant, and it does not change over arc length and only related with the wire stem elongation [17]. In the pulsed arc welding process, the welding wire melting rate during peak pulse current is greater than the wire feed speed, the wire stem elongation decreases, and the pulse current base value during welding wire melting rate is less than the wire feed speed, the wire stem elongation increase, but in the whole pulse current cycle only the tiniest cyclical fluctuations, wire stem elongation, and arc length relative change, as shown in Figure 2.

At 2 s in the simulation model, the welding torch suddenly drops from 40 mm height to 30 mm height, as shown in Figure 3. Due to the constant dry elongation of welding wire, the arc length is bound to change abruptly, changing from about 16 mm before the step to about 6 mm, which is basically equal to the step change distance. After the step change of the distance between the conductive tip and the weldment occurs, the voltage drop of the dry elongation of the welding wire remains unchanged, as shown in Figure 3. Therefore, it can be seen that in the process of fixed-frequency arc welding, in the case of constant wire feeding speed, the shake of the welding torch and the unevenness of the weldment surface may lead to a step change of arc length. To maintain the stability of the arc welding process, it is difficult to adopt the control of fixed-frequency pulse current waveform. In order to improve the disturbance adaptability of pulse welding, pulse frequency modulation (PFM), and adaptive adjustment of pulse current related parameters can effectively eliminate the interference factors in the welding process, quickly adjusting arc welding parameters to make the welding wire melting speed equal to the wire feeding speed, maintaining the stability of the welding process, and improving the weld forming effect [18].

Through the software programming, the current and voltage signal with noise are first processed by wavelet filtering, and then the input energy, dynamic resistance, U-I graph analysis, statistical analysis, etc., to obtain simple and clear charts, so as to analyze and evaluate the dynamic characteristics of the welding arc.

In order to dynamically adjust the welding parameters and form a closed-loop control system software in the arc welding process, arc pressure control is usually adopted. When arc dynamic changes in arc length cause arcing voltage changes, this change as the input signal of the electric arc voltage feedback controller and automatically by the arc welding of the adjustment system control algorithm, forced

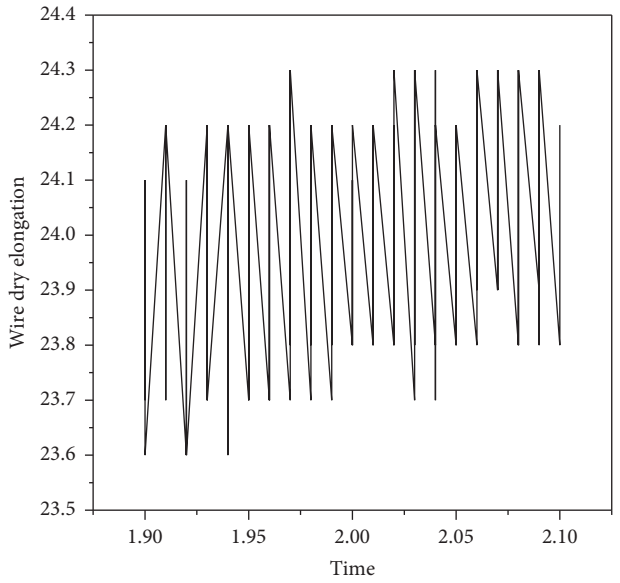

Figure 2: Change curve of wire dry elongation.

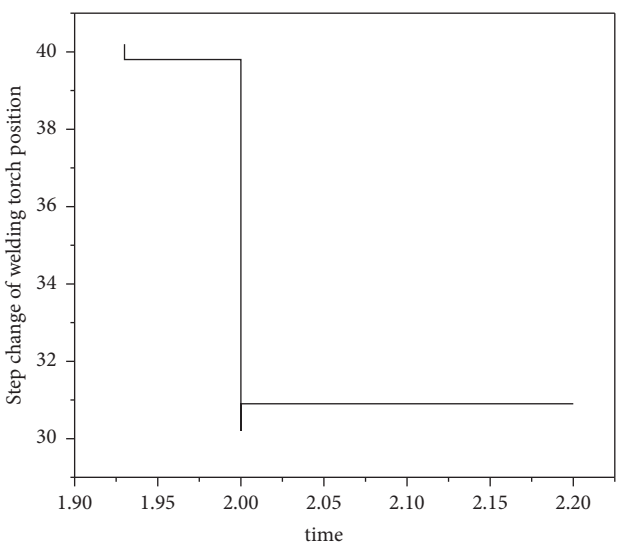

Figure 3: Step change curve of the distance between conductive tip and weldment.

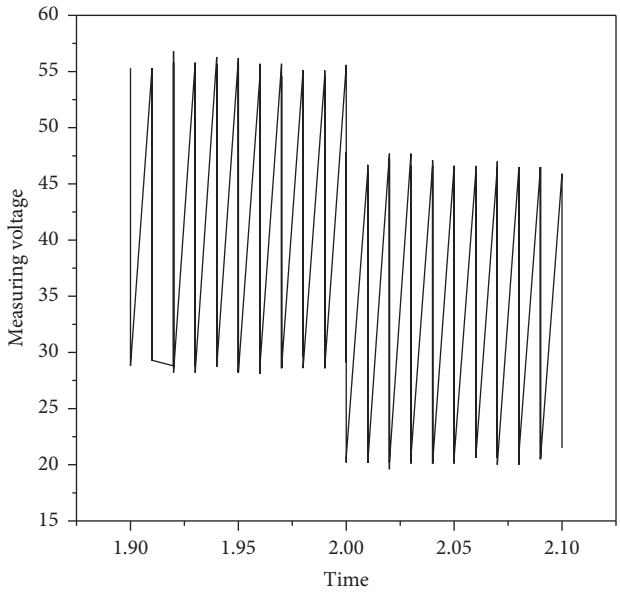

Figure 4: Century sampling voltage curve.

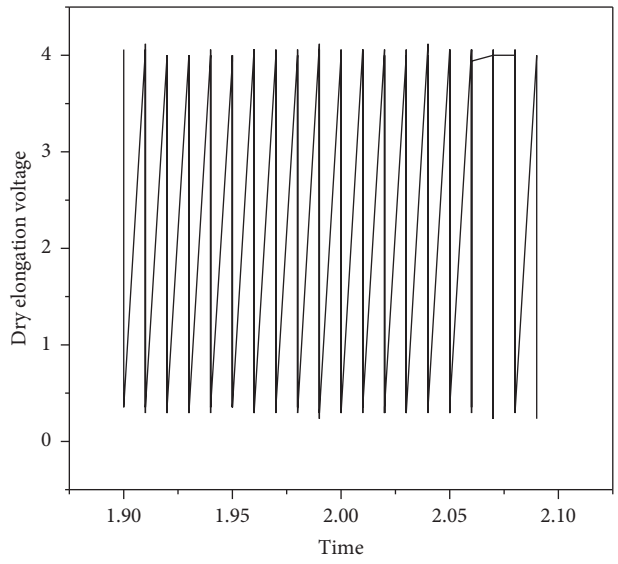

Figure 5: Pressure drop curve of wire dry elongation.

to adjust the parameters of pulse current, through dynamic adjustment process of a very short time, making the wire melting rate is equal to the wire feed speed; to restore arc length, arc welding process is kept dynamic and smooth. In order to sample the arc voltage, a voltage sensor is usually installed at the position of the conductive tip for the convenience of installation. Since the voltage signal collected by the sensor at the position of the conductive tip includes the actual arc voltage value and the voltage drop of the dry elongation of the welding wire, as shown in Figure 4. It can be seen from Figures 4 and 5 that the voltage drop of wire dry elongation is one order of magnitude smaller than the sampling voltage signal, and the change of dry elongation voltage drop is relatively stable. Therefore, it is generally considered feasible to sample voltage from the conductive nozzle as the arc voltage feedback signal [19, 20].

4. Conclusions

Through the optimization of the pulse control subroutine, the control of the system software reduces the impact and increases the response speed and control accuracy. The arc length control method can be studied by expert neural network algorithm, model reference adaptive control algorithm, robust control algorithm, and internal model control algorithm, and the arc simulation model established can be optimized. Since the modeling of soft switch pulse GMAW welding inverter power supply is based on some simplification, other research methods are necessary to

further study the mathematical model of soft switch pulse GMAW welding inverter power supply and establish a more accurate system model to guide the parameter design of arc welding power supply.

Data Availability

The data used to support the findings of this study are available from the corresponding author upon request.

Conflicts of Interest

The authors declare that they have no conflicts of interest.

References

[1] C. Li, B. Yuan, J. Ren, L. Sun, and J. Wang, "Research on optimization of charge batch planning based on augmented Lagrangian relaxation algorithm," *IFAC-PapersOnLine*, vol. 52, no. 1, pp. 814–819, 2019.

[2] H. Wei, Z. Qian, Q. Bo, and Y. Yang, "Research on hs optical flow algorithm based on motion estimation optimization," *Journal of Computer and Communications*, vol. 6, no. 11, pp. 171–184, 2018.

[3] M. E. A. Elaziz, A. A. ElGhany Ewees, and Z. Alameer, "Improving adaptive neuro-fuzzy inference system based on a modified salp swarm algorithm using genetic algorithm to forecast crude oil price," *Natural Resources Research*, vol. 29, no. 4, pp. 2671–2686, 2020.

[4] M. M. Hu, Y. Zhang, and S. W. Yuan, "Research and application of milling parameters optimization based on genetic algorithm," *Advanced Materials Research*, vol. 1095, pp. 820–823, 2015.

[5] Z. Li and K. Chen, "Research on timing optimization of reginal traffic signals based on improved genetic algorithm," *IOP Conference Series: Materials Science and Engineering*, vol. 423, no. 1, Article ID 012191, 2018.

[6] L. Peng and W. Li, "Research on optimization method of power communication based on topological algorithm," *Clinica Chimica Acta*, vol. 42, no. 2, pp. 605–609, 2017.

[7] J. Liu and Q. Feng, "Research on anti-collision algorithm optimization of rfid tag based on binary search," *Revista de la Facultad de Ingenieria*, vol. 32, no. 6, pp. 15–22, 2017.

[8] J. H. Lim and T. S. Kim, "Optimization of information security investment portfolios based on data breach statistics: a genetic algorithm approach," *Information Systems Review*, vol. 22, no. 2, pp. 201–217, 2020.

[9] L. X. Jin, Q. X. Feng, and Z. F. Pan, "Slope stability analysis based on morgenstern-price method and improved radial movement optimization algorithm," *Zhongguo Gonglu Xuebao/China Journal of Highway and Transport*, vol. 31, no. 2, pp. 39–47, 2018.

[10] A. Mhdawi and H. S. Al-Raweshidy, "A smart optimization of fault diagnosis in electrical grid using distributed software-defined iot system," *IEEE Systems Journal*, vol. 14, no. 1, pp. 2780–2790, 2020.

[11] A. Eshaghzadeh and A. Hajian, "Multivariable modified teaching learning based optimization (mm-tlbo) algorithm for inverse modeling of residual gravity anomaly generated by simple geometric shapes," *Journal of Environmental & Engineering Geophysics*, vol. 25, no. 4, pp. 463–476, 2020.

[12] Z. Liu, P. Yang, D. Li, and M. Xu, "Sliding mode prediction fault-tolerant control method based on whale optimization algorithm," *International Journal of Innovative Computing Information and Control*, vol. 15, no. 6, pp. 2119–2133, 2019.

[13] L. Chaoming, "Prediction and analysis of sphere motion trajectory based on deep learning algorithm optimization," *Journal of Intelligent and Fuzzy Systems*, vol. 37, no. 5, pp. 6275–6285, 2019.

[14] X. Bi and C. Yan, "Constrained optimization algorithm based on double populations," *Journal of Harbin Institute of Technology*, vol. 23, no. 2, pp. 66–71, 2016.

[15] G. R. Zhu, Z. Liu, X. Li, B. Y. Liu, S. X. Duan, and Y. Kang, "Research on digital soft switch welding/cutting inverter power source," in *Proceedings of the 2007 7th International Conference on Power Electronics and Drive Systems*, pp. 325–329, Bangkok, Thailand, April 2007.

[16] M. Behnasr and H. Jazayeri Rad, "Robust data-driven soft sensor based on iteratively weighted least squares support vector regression optimized by the cuckoo optimization algorithm," *Journal of Natural Gas Science and Engineering*, vol. 22, pp. 35–41, 2015.

[17] Z. Lu, X. Li, Q. Chen, and X. Zou, "Kalman filtering decoupling algorithm based on particle swarm optimization," *Xi Tong Gong Cheng Yu Dian Zi Ji Shu/Systems Engineering and Electronics*, vol. 40, no. 4, pp. 751–755, 2018.

[18] E. V. Yagup, "An active power filter at operation on the unbalanced and nonlinear loads with control by optimization algorithm," *Electrical Engineering & Electromechanics*, vol. 0, no. 5, pp. 23–26, 2017.

[19] Z. Xinting, K. Lei, W. Qianqian, Z. Wanyi, and L. Yuyao, "Psd nonlinear correction based on bp optimization algorithm," *Journal of Applied Optics*, vol. 37, no. 3, pp. 415–418, 2016.

[20] Z. Guan and Y. Zhang, "Terrain quadtree segmentation algorithm optimization based on near space platform," *Nanjing Hangkong Hangtian Daxue Xuebao/Journal of Nanjing University of Aeronautics and Astronautics*, vol. 47, no. 1, pp. 59–63, 2015.